ACS EARTH AND SPACE CHEMISTRY

http://pubs.acs.org/journal/aesccq

Article

Infrared Spectra and Intensities of Amorphous and Crystalline Allene

Reggie L. Hudson* and Yukiko Y. Yarnall

Cite This: *ACS Earth Space Chem.* 2022, 6, 1163−1170

Read Online

ACCESS | Metrics & More | Article Recommendations

ABSTRACT: The infrared (IR) spectra, including spectral intensities, of solid hydrocarbons are of interest to astrochemists and astronomers for the relevance of these compounds to surface chemistry in the outer solar system and beyond. However, although the vibrational modes and IR peak positions of many such compounds have long been studied, much less attention has been paid to the IR intensities needed to quantify both astronomical observations and laboratory results. Here we present mid- and near-IR transmission spectra of a relatively little-studied solid hydrocarbon, allene (1,2-propadiene). Spectra of both amorphous and polycrystalline allene are shown for the first time along with optical constants, band strengths, and absorption coefficients. We also report a density and refractive index (670 nm) for each form of solid allene. A radiation-chemical experiment on allene's formation is described, as are some applications and suggestions for future work.

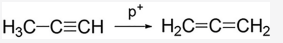

KEYWORDS: *IR spectroscopy, band strengths, astrochemistry, amorphous solids, ices*

1. INTRODUCTION

Observations of objects in the outer Solar System and of interstellar grains have revealed the presence of a number of icy solids, such as frozen CH_4, CO, and H_2O. Stellar vacuum ultraviolet photons, magnetospheric radiation, and cosmic rays act on these ices to generate more complex molecules, such as C_2H_6 from CH_4, CO_2 from CO, and H_2O_2 from H_2O. Infrared (IR) spectroscopy has proven to be the major analytical tool for the study of these molecules in the solid state within the Solar System and in ices of the interstellar medium. For such work, reference IR spectra of solid samples under vacuum at low temperatures are needed. Such data would ideally include not only careful documentation of spectral positions but also spectral intensities from which molecular abundances can be determined. However, despite extensive studies of many icy solids in recent decades, the measurement of IR intensities, such as band strengths, remains far behind the recording of IR spectra.

In this paper, we continue our recent work on IR intensities of solids relevant to planetary and interstellar hydrocarbon ices. So far we have examined solid methane (CH_4), ethane (C_2H_6), ethylene (C_2H_4), and acetylene (C_2H_2) in amorphous and crystalline forms,[1−3] and more recently we investigated solid propane (C_3H_8), propylene (C_3H_6), and propyne (C_3H_4).[4] Here we turn to allene (1,2-propadiene, $H_2C{=}C{=}CH_2$), which is present in the atmosphere of Titan, Saturn's largest moon.[5] Investigations of allene's vibrational spectrum have a long history reaching back to at least the 1930s.[6] Early researchers identified most of allene's fundamental vibrations using both IR and Raman methods, with analyses of rotational fine structure leading to rotational constants, moments of inertia, and molecular dimensions for the gas-phase molecule.[7] The earliest study of solid allene appears to have been that of three single crystals by Blanc et al., who also published liquid- and gas-phase results.[8] In the nearly 60 years since then, studies of allene's IR spectrum have continued to address positions, anharmonicites, and spectral intensities, among other topics, but it is with this last property, IR intensities, that investigations of solid allene and gas-phase allene have diverged. Despite an interest in allene IR intensities by both laboratory astrochemists and astronomical observers, quantitative intensity results are lacking for the solid phase of the compound at cryogenic temperatures. In this paper, we report the first such intensity measurements on two solid forms of allene. With our new IR results it is now possible to make ices of known allene concentrations for quantitative IR work.

2. EXPERIMENTAL SECTION

Allene was purchased from Sigma-Aldrich (MilliporeSigma) and used as received. Our allene spectra showed no trace of a propyne impurity at 3300 cm^{-1}. Allene ices were made with standard vacuum-line methods by deposition onto a precooled KBr substrate within a vacuum system (10^{-8} Torr). A "shower-head" array, or other, disperser was used to help produce a uniform ice on the substrate. The deposition rate was such as to give an increase in the ice sample's thickness of a few micrometers per hour, as measured by interference fringes. Measurements for IR spectra and the corresponding

Special Issue: Chemical Complexity in Planetary Systems

Received: September 29, 2021
Revised: March 29, 2022
Accepted: March 31, 2022
Published: April 19, 2022

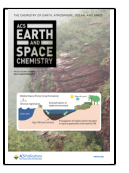

interference fringes were made in transmission through the substrate. See the paper of Moore et al. for two diagrams.[9]

Fringe patterns resembled those in previous publications from our group.[10] At no time under any conditions of temperature or deposition rate was a fringe pattern observed that would indicate unusual deposition on two sides of the substrate.[11]

The thickness (h) of each ice was determined with eq 1 where N_{fr} is the number of interference fringes recorded during the sample's deposition and $\theta = 3.57 \pm 0.04°$ was the angle between the incident beam from a 670 nm laser and a line drawn perpendicular to the substrate.

$$h = \frac{N_{fr}\lambda}{2\sqrt{{n_{670}}^2 - \sin^2\theta}} \quad (1)$$

Here n_{670} is the ice sample's refractive index at 670 nm, which was measured in a separate experiment by two laser interferometry. See below and our recent papers for more details, or consult original work by Heavens,[12] Tempelmeyer and Mills,[13] and Groner et al.[14]

Infrared spectra were recorded in a conventional transmission mode with an interfaced Thermo iS50 FTIR spectrometer set for 200 scans per spectrum and a resolution of either 0.5 or 1 cm^{-1} from 7000 to 400 cm^{-1}. Spectra shown here are with the lower resolution (1 cm^{-1}), but calculations were with the higher resolution (0.5 cm^{-1}) data. In practice, the higher resolution did not change either band areas or peak heights but did increase baseline noise in some cases.

To determine IR band strengths we needed to have each ice sample's density (ρ), and to get a thickness a reference refractive index was required, as seen in eq 1. These were determined in a UHV chamber ($P \sim 10^{-10}$ Torr) with a quartz crystal microbalance to get ρ and with two laser interferometry to get a refractive index at 670 nm (n_{670}). See our recent papers for details.[10]

A few measurements were made of the IR spectrum of solid propyne ($H_3C{-}C{\equiv}CH$, methyl acetylene), again obtained from Sigma-Aldrich. For amorphous propyne, a band strength of $A'(C{\equiv}C, 2124\ cm^{-1}) = 4.69 \times 10^{-19}$ cm molecule^{-1} was obtained at ~10 K using the same methods and equipment as in our allene work, and as described in the following section. See Hudson et al. for full results on propyne.[4]

3. RESULTS

3.1. Densities and Refractive Indices. Infrared spectra (*vide infra*) showed that an amorphous ice was produced when allene was deposited on our KBr substrate that had been precooled to between 8 and about 45 K. Few differences were found in the IR spectra of allene deposited at these temperatures, but higher-temperature depositions gave crystalline allene. Warming any allene ice to 100 K resulted in its loss by sublimation in only a few minutes. These observations helped guide our determinations of densities and refractive indices for allene ices.

We measured n_{670} and ρ for amorphous allene at 19 K, the base temperature of our UHV cryostat, and obtained $n_{670} = 1.459 \pm 0.003$ and $\rho = 0.735 \pm 0.002$ g cm^{-3}, where the uncertainties are standard errors based on measurements made in triplicate. Depositions at 55 K for crystalline allene gave $n_{670} = 1.565 \pm 0.005$ and $\rho = 0.867 \pm 0.004$ g cm^{-3}. These latter two values scarcely changed at higher temperatures, but the fringe patterns were less uniform. Weak or unusual behavior in fringe patterns for allene has been described in a technical report, but not in the peer-reviewed literature.[15]

3.2. Infrared Spectra. Infrared spectra of allene deposited at 8 K are shown in Figures 1−5. The overall appearance of

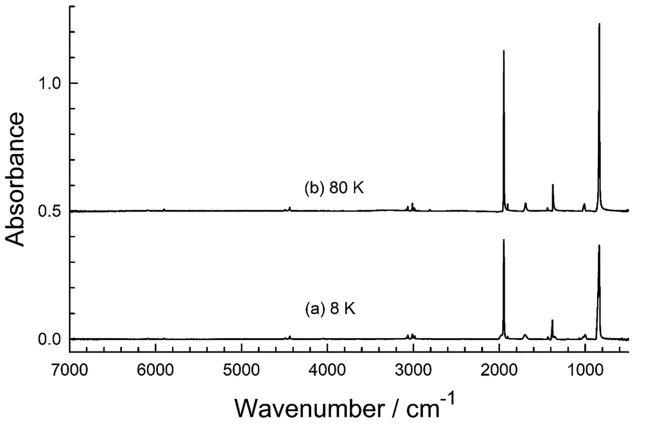

Figure 1. Infrared survey spectra of allene deposited at (a) 8 K for a thickness of about 0.92 μm and (b) deposited at 80 K for a thickness of about 0.86 μm. Spectra are offset for clarity.

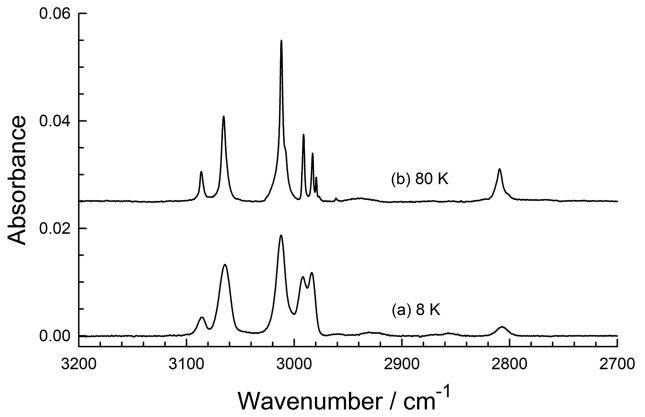

Figure 2. Infrared spectra of allene deposited at (a) 8 K for a thickness of about 0.92 μm and (b) deposited at 80 K for a thickness of about 0.86 μm. Spectra are offset for clarity.

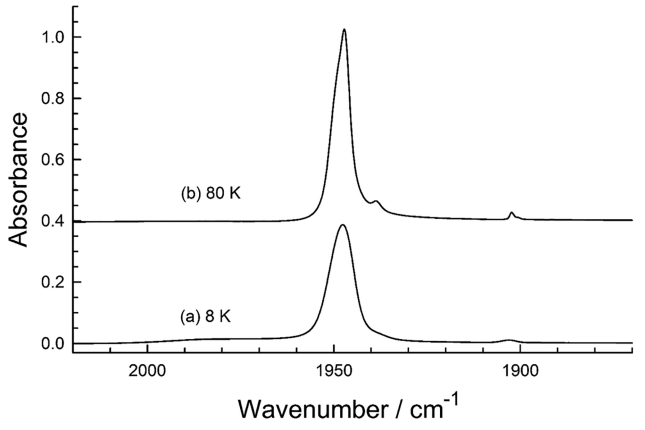

Figure 3. Infrared spectra of allene deposited at (a) 8 K for a thickness of about 0.92 μm and (b) deposited at 80 K for a thickness of about 0.86 μm. Spectra are offset for clarity.

https://doi.org/10.1021/acsearthspacechem.1c00339
ACS Earth Space Chem. 2022, 6, 1163−1170

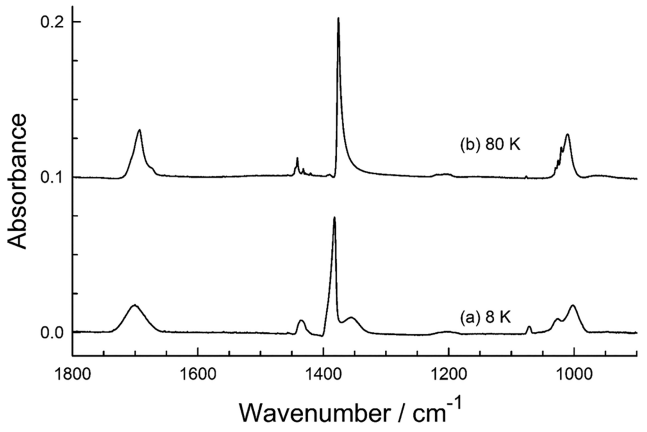

Figure 4. Infrared spectra of allene deposited at (a) 8 K for a thickness of about 0.92 μm and (b) deposited at 80 K for a thickness of about 0.86 μm. Spectra are offset for clarity.

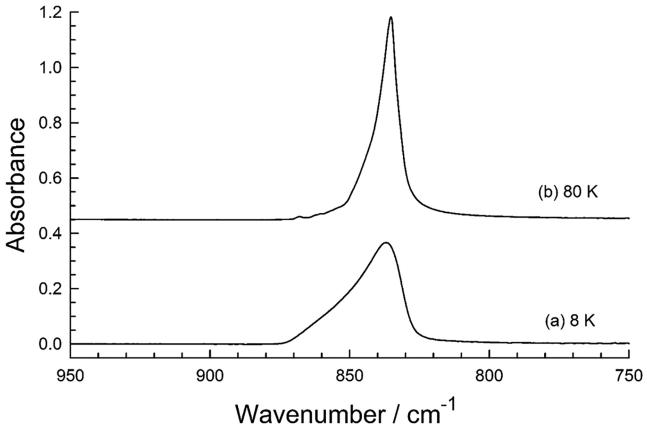

Figure 5. Infrared spectra of allene deposited at (a) 8 K for a thickness of about 0.92 μm and (b) deposited at 80 K for a thickness of about 0.86 μm. Spectra are offset for clarity.

spectrum (a) in each figure is as expected from the limited amount of published work on solid allene. Our 8 K spectrum is dominated by intense absorbances at 1947 and 837 cm^{-1}, the latter showing the pronounced asymmetry of an inhomogeneously broadened feature. Trace (a) in each figure shows the rounded features characteristic of an amorphous ice.[16] In contrast, trace (b) in each figure shows that the spectrum of an ice made at 80 K had bands that were somewhat sharper than at the lower temperature. For example, see peaks near 3000 and 1000 cm^{-1}. The changes were attributed to ices being crystalline at 80 K. The latter peak was confirmed by warming a sample made at 8 K to 80 K and comparing the resultant spectrum to that of an ice made by deposition at 80 K. Table 1 gives solid-phase positions corresponding to most of allene's fundamentals, with comparisons to gas-phase values. In practice, few changes with temperature were seen in amorphous allene's spectrum until the ice was crystallized, and few changes were seen thereafter until the ice sublimed.

To measure IR intensities, we proceeded as in our recent work on, for example, acetone and dimethyl ether.[17,18] Spectra of ices at multiple thickness were recorded, and the heights (absorbances) of selected peaks and the areas of selected bands were measured. Appropriate Beer's law plots were constructed of height and area as a function of ice thickness from which

Table 1. Mid-IR Absorptions of Allene

symmetry species[a]	no.	approximate description[a]	$\tilde{\nu}$ gas-phase/ cm^{-1}	$\tilde{\nu}$ amorphous/ cm^{-1}	$\tilde{\nu}$ crystalline/ cm^{-1}
a_1	1	C−H stretch	2996	2992	2991
a_1	2	CH_2 bend	1440	1435	1441
a_1	3	CCC symm stretch	1076	1072	–[b]
b_1	4	CH_2 torsion	865	–[b]	–[b]
b_2	5	C−H stretch	3005	3012	3012
b_2	6	CCC asymm stretch	1957	1947	1947
b_2	7	CH_2 bend	1398	1382	1376
e	8	C−H stretch	3085	3064	3066
e	9	CH_2 rock	1015	1002	1011
e	10	CH_2 rock	842	837	835
e	11	CCC bend	354	–[b]	–[b]

[a]Symmetries, numbers, approximate descriptions, and gas-phase positions are from the work of Lord and Venkateswarlu.[7] See also Blanc et al.[8] [b]Not observed or very weak; see text.

apparent absorption coefficients (α') and apparent band strengths (A') were calculated from slopes using eqs 2 and 3.

$$\ln(10) \times (\text{absorbance of peak}) = \alpha' h \quad (2)$$

$$\ln(10) \times \int_{\text{band}} (\text{absorbance}) d\tilde{\nu} = (\rho_N A') h \quad (3)$$

See Hollenberg and Dows and our earlier papers for details.[19] In eq 3, ρ_N is the ice sample's number density, in molecules cm^{-3} in this paper. Deposition temperatures were 8 and 80 K for amorphous and crystalline ices, respectively, and at least five thicknesses were used for each determination of α' or A'. Correlation coefficients were 0.999 and higher, except for a few near-IR features that were about 0.998 and higher. Final results for α' and A' are given in Tables 2 and 3 for selected IR peaks and bands.

Table 2. Intensities of Selected Mid-IR Absorptions of Amorphous Allene at 8 K

$\tilde{\nu}/cm^{-1}$	α'/cm^{-1}	integration range/cm^{-1}	$A'/10^{-18}$ cm $molecule^{-1}$
3064	329 ± 3	3100−3035	0.442 ± 0.004
3012	451 ± 5	3035−2960	0.880 ± 0.009
1947	9060 ± 91	2010−1910	8.74 ± 0.087
1702	388 ± 4	1750−1650	1.31 ± 0.013
1382	1660 ± 17	1405−1320	2.15 ± 0.021
1002	339 ± 3	1060−960	1.00 ± 0.010
837	7720 ± 77	880−810	16.4 ± 0.164

Table 3. Intensities of Selected Mid-IR Absorptions of Crystalline Allene at 80 K

$\tilde{\nu}/cm^{-1}$	α'/cm^{-1}	integration range/cm^{-1}	$A'/10^{-18}$ cm $molecule^{-1}$
3066	427 ± 17	3077−3053	0.153 ± 0.005
3012	909 ± 36	3027−3000	0.428 ± 0.013
1947	15600 ± 624	1965−1930	8.38 ± 0.251
1692	1000 ± 40	1730−1650	1.47 ± 0.044
1376	3080 ± 123	1384−1334	2.31 ± 0.069
1011	669 ± 27	1045−990	0.923 ± 0.028
835	16300 ± 653	865−805	13.3 ± 0.399

https://doi.org/10.1021/acsearthspacechem.1c00339
ACS Earth Space Chem. 2022, 6, 1163−1170

Uncertainties in α' and A' were estimated with both a propagation-of-error approach and a least-squares routine, taking into consideration uncertainties in both x and y quantities in the slopes of the Beer's law plots corresponding to eqs 2 and 3.[20,21] For amorphous allene, uncertainties in α' and A' were near 1% for mid-IR features ($\tilde{\nu} \leq 4000$ cm^{-1}) and about 3 and 7% in α' and A', respectively, for near-IR absorbances ($\tilde{\nu} \geq 4000$ cm^{-1}). For crystalline allene, uncertainties in α' and A' were about 4% for mid-IR features and about 7 and 11%, respectively, for near-IR absorbances. As expected, the uncertainties in both α' and A' were greater for the near-IR region than the mid-IR. These uncertainties compare well to values in the literature, such as from Hudgins et al.[22] and Luna et al.,[23] but they could be reduced even more by additional measurements.

Infrared features other than those in our tables, mostly for smaller bands, also were present in our allene spectra, but for the most part they were ignored except for checking against earlier work. For example, we found overtone and combination bands near 2807 ($\nu_2 + \nu_7$), ~1700 ($2\nu_{10}$, $\nu_4 + \nu_{10}$), 1356 ($\nu_9 + \nu_{11}$), and 1203 ($\nu_{10} + \nu_{11}$) cm^{-1} in the spectrum of amorphous allene. See Blanc et al. for more on these assignments.[8] The small peak near 1903 cm^{-1} appears to be a ^{13}C satellite of the intense ν_3 peak at 1947 cm^{-1}.

Going beyond the mid-IR region, Figure 6 shows near-IR features of solid allene. The sharp peaks near 6092 (1.64 μm, $2\nu_8$), 5900 (1.69 μm, $\nu_1 + \nu_5$), 4490 (2.23 μm, $\nu_2 + \nu_8$), and 4438 cm^{-1} (2.25 μm, $\nu_2 + \nu_7$) could be useful in the search for solid allene in the spectra of icy satellites, and so we have measured those peaks' intensities. Results are in Tables 4 and 5, where wavelengths also are given as they are often used by observational astronomers.

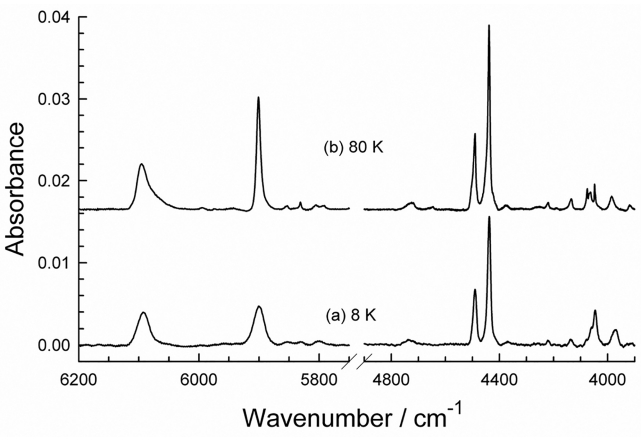

Figure 6. Infrared spectra of allene deposited at (a) 8 K for a thickness of about 0.92 μm and (b) deposited at 80 K for a thickness of about 0.86 μm. Spectra are offset for clarity.

Table 4. Four Near-IR Absorptions of Amorphous Allene at 8 K

$\tilde{\nu}$/cm^{-1}	λ/μm	α'/cm^{-1}	integration range/cm^{-1}	$A'/10^{-18}$ cm molecule^{-1}
6092	1.64	68 ± 5	6135–5986	0.170 ± 0.005
5900	1.69	77 ± 5	5986–5868	0.190 ± 0.006
4490	2.22	107 ± 8	4520–4470	0.153 ± 0.005
4438	2.25	262 ± 18	4470–4400	0.369 ± 0.011

Table 5. Four Near-IR Absorptions of Crystalline Allene at 80 K

$\tilde{\nu}$/cm^{-1}	λ/μm	α'/cm^{-1}	integration range/cm^{-1}	$A'/10^{-18}$ cm molecule^{-1}
6095	1.64	96 ± 11	6135–6010	0.220 ± 0.015
5900	1.69	241 ± 27	5920–5868	0.183 ± 0.013
4490	2.22	153 ± 17	4520–4470	0.159 ± 0.011
4438	2.25	383 ± 42	4470–4400	0.387 ± 0.027

3.3. Optical Constants. Optical constants of ices are used in computational models of icy surfaces in the Solar System, and to that end we calculated the real and imaginary components, $n(\tilde{\nu})$ and $k(\tilde{\nu})$, respectively, of solid allene's complex index of refraction. Our calculations of optical constants used an iterative Kramers–Kronig routine that ended when the calculated $n(\tilde{\nu})$ and $k(\tilde{\nu})$ values produced a spectrum with intensities (i.e., peak heights) that matched those of the experimental spectrum to within 1 part in 10^5 at every wavenumber. The main initial uncertainty in the computation was with the thickness of an ice sample, an issue that we addressed by measuring the reference refractive indices already mentioned and used in eq 1. Moreover, our standard procedure is to calculate optical constants for ices of multiple thicknesses (typically a minimum of five) at each temperature chosen and to average the resulting n and k values at each wavenumber. This avoids the need to rely on the IR spectrum, the measured thickness, and the results from a single allene ice. In short, the uncertainties in our optical constants amount to no more than 1 part in 10^5 at any wavenumber when compared to measured spectra. For additional information about our computer routine, developed by one of our colleagues (P. A. Gerakines), see the paper of Gerakines and Hudson.[24]

Figure 7 shows, as an example, the optical constants we calculated for amorphous allene. The values plotted are available in an electronic version on our group's web page at https://science.gsfc.nasa.gov/691/cosmicice/ along with corresponding results for crystalline allene.

3.4. An Application—Allene Formation. Isomerizations at low temperatures are one of our group's interests, such as the conversion of propyne into allene and *vice versa*. However, the coronavirus pandemic closed our laboratory and prevented all but one exploratory experiment, which we wish to put on record here. Our experiment was the radiation-induced HC≡C—CH_3 → H_2C=C=CH_2 isomerization near 20 K, the radiation source being 1 MeV H^+ from a Van de Graaff accelerator with a beam current of ~1 × 10^{-7} A.

Trace (a) in Figure 8 is an expansion of the spectrum of solid propyne at 20 K, with the large peak on the left near 2123 cm^{-1} being from propyne's C≡C stretch. Spectrum (b) is from the same sample after a radiation dose of about 10 eV molecule^{-1}. The C≡C peak on the left has decreased and a peak near 1948 cm^{-1} has increased, a peak we assign to allene (Table 1). Warming the irradiated sample above ~100 K removed both the residual propyne and the allene product, as expected. Spectrum (b) in Figure 8 also shows that IR features were produced near 1948 cm^{-1} other than for allene. These can be assigned to reaction products of propyne and allene, probably from polymerization. From the decrease in the propyne feature near 2123 cm^{-1} and the increase in the allene feature near 1948 cm^{-1}, and the strength (A') of each IR band, we estimate that about 10% of the propyne sample underwent

https://doi.org/10.1021/acsearthspacechem.1c00339
ACS Earth Space Chem. 2022, 6, 1163–1170

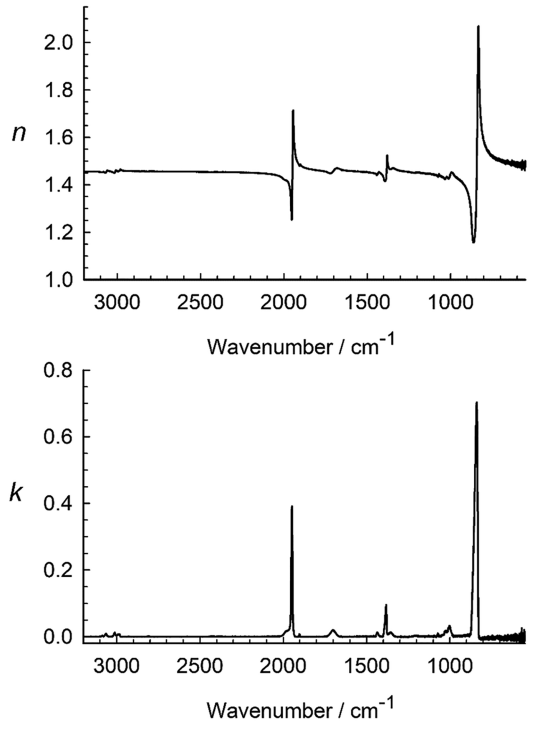

Figure 7. Optical constants of amorphous allene at 8 K.

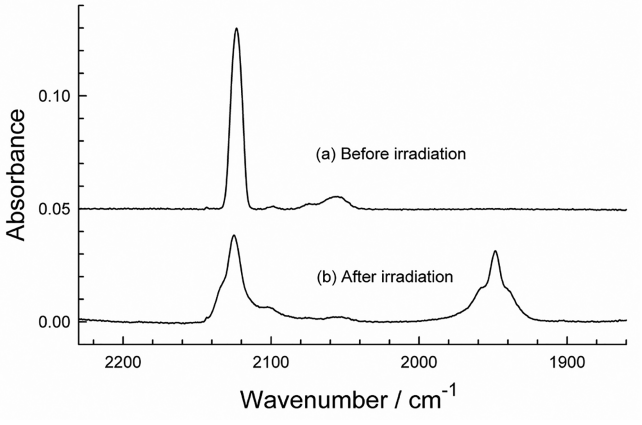

Figure 8. Spectrum of propyne (methyl acetylene) before and after irradiation to a dose of about 10 eV molecule^{-1} at 20 K. The thickness of the ice in (a) was about 1 μm. Spectra are offset for clarity.

the HC≡C—CH_3 → H_2C=C=CH_2 isomerization. Admittedly, the experiment is barely above the proof-of-concept level, and the estimate of reaction yield is rough, but Figure 8 shows that ionizing radiation initiates the propyne-to-allene isomerization. Extensions to other temperatures and ice compositions (e.g., inclusion of H_2O ice) should be straightforward.

4. DISCUSSION

4.1. Densities and Refractive Indices. We have not found previous measurements of either n_{670} or ρ for solid allene under conditions similar to ours. Blanc et al. reported ρ = 0.86 g cm^{-3} for crystalline allene made by cooling a liquid sample, close to our ρ = 0.867 g cm^{-3} for an ice made by vapor-phase deposition.[8] As a check on our work, we used our n_{670} and ρ results to calculate molar refractions (R_M) for amorphous and crystalline allene, expecting near identical values for the two forms of the compound. We found R_M = 14.9 and 15.0 cm^3 mol^{-1} for amorphous and crystalline allene, respectively, which is less than a 1% difference.

4.2. Infrared Spectra. A gas-phase allene molecule is a prolate symmetric top belonging to the D_{2d} point group with $3N - 6 = 3(7) - 6 = 15$ fundamental vibrations distributed among four different symmetry species as $\Gamma_{red} = 3a_1 + b_1 + 3b_2 + 4e$. Of these, the 7 b_2 and doubly degenerate e motions, constituting 11 vibrations, are IR active in the gas phase. Our IR spectra show evidence for 12 vibrations in the solid, the missing three being a type e mode in the far-IR (~350 cm^{-1}) beyond our spectral reach, and a weak type b_1 feature on the side of the large band near 840 cm^{-1}. Our Tables 2 and 3 list results for some of the stronger and better resolved IR features of allene, which were chosen to cover a large portion of the mid-IR region with an eye toward avoiding prominent bands of other, more abundant extraterrestrial molecules.

Allene's C=C=C symmetric stretch (ν_3) in Table 1 is formally IR forbidden in the gas phase, but not necessarily forbidden in condensed phases. Trace (a) of Figure 4 shows a weak band at 1070 cm^{-1} for this vibration in amorphous allene at 8 K. However, this feature is barely perceptible in trace (b) for the crystalline ice made by deposition at 80 K. This behavior is similar to our observations of nominally forbidden features in the IR spectra of other amorphous solids such as CH_4 (2904 cm^{-1}), C_2H_6 (993 cm^{-1}), C_2H_4 (1618 cm^{-1}), C_2H_2 (1961 cm^{-1}), CO_2 (1384 cm^{-1}), C_2N_2 (849 cm^{-1}), and also the ammonium ion NH_4^+ (1680 cm^{-1}) in NH_4SH.[1−3,9,25,26] In each case, the nominally forbidden peak was not seen in the corresponding crystalline solid. This relaxation or loss of selection rules can be traced back to at least the 1940s, and so is by no means new or novel with our work.[27]

Our IR spectra of amorphous allene at 8 K are qualitatively similar to the spectrum of liquid allene at 140 K published by Blanc et al., although their spectrum's more intense features appear to be saturated, hindering quantitative comparisons.[8] Those same authors recorded spectra of polycrystalline allene, but none were shown. Several measurements of gas-phase allene's mid-IR intensities have been published, and are in reasonable agreement with each other.[28] The two strongest peaks in our allene spectra, near 1947 and 837 cm^{-1}, are also the strongest in the gas-phase data, but with our intensities being ~15% higher than the gas-phase values. Table 6 compares the intensities of the asymmetric stretching vibrations of the 16 electron isoelectronic molecules CO_2, N_2O, and allene, each with cumulated bonding. For the gas phase, the trend A'(CO_2, 2349 cm^{-1}) > A'(N_2O, 2224 cm^{-1}) > A'(allene, 1957 cm^{-1}) is found, and this same trend holds for the crystalline and amorphous forms of these three compounds. In each case, allene is the weakest absorber. See

Table 6. IR Band Strengths (A'/10^{-18} cm molecule^{-1}) of Three Forms of Three Compounds[a]

form	O=C=O	O=N=N	H_2C=C=CH_2
gas	109.6	60.8	8.58
crystalline	76.4	39.8	8.38
amorphous	118	58.9	8.74

[a]Each band strength is for the asymmetric vibration about the molecule's central atom. See the text for references and positions.

https://doi.org/10.1021/acsearthspacechem.1c00339
ACS Earth Space Chem. 2022, 6, 1163−1170

Yamada and Person for data on gas-phase and crystalline CO_2 and N_2O,[29] see Es-sebbar et al. for gas-phase allene data,[28] and see our earlier papers and the present work for the remaining entries in Table 6.[10,25]

The band shapes of our allene spectra are such that widths of the amorphous ice features are somewhat greater than for IR spectra of crystalline samples, but not dramatically so in most cases. Perhaps the most interesting band shape is that of the intense feature near 837 cm^{-1} in amorphous allene, a strongly asymmetric shape that is indicative of inhomogeneous broadening.[30−32] We have found the same strong asymmetry of trace (a) in Figure 5 in the IR bands of other molecules of 16 valence electrons with cumulated bonding, such as CO_2 (655 cm^{-1}),[25] OCS (2020 cm^{-1}),[33] and N_2O (2221 cm^{-1}).[10] For spectra of other hydrocarbons with similar broadening, see solid CH_4 (1297 cm^{-1}),[1,26] C_2H_6 (817 cm^{-1}),[2] and C_2H_2 (742 cm^{-1}).[3] A strongly asymmetric band also has been reported for the 1040 cm^{-1} feature of amorphous ozone.[34]

As an aside, we note that we did not encounter any problems preparing amorphous allene by vapor-phase deposition and recording its IR spectrum. This contrasts with difficulties we met in preparing amorphous solids from the smaller molecules CO_2 and N_2O, allene's isoelectronic counterparts in Table 6.[10,25] We also have found it more difficult to prepare amorphous ices from the simplest alkane, alkene, and alkyne (i.e., CH_4, C_2H_4, and C_2H_2) than from the next member of each class (i.e., C_2H_6, C_3H_6, and C_3H_4).[1−4] Similarly, Mizuno et al. described difficulties in preparing amorphous CO_2 even at 3 K, and Takeda et al. had difficulty making amorphous C_2H_4 by deposition at 4.2 K.[35,36]

We suggest that such problems in preparing amorphous solids and acquiring their IR spectra arise largely from the deposition rate used to make solid samples, and the accompanying energy release. Some years ago, Jacox noted that "appreciable heat is given off when a gaseous sample is condensed" onto a cold window.[37] Even earlier, Fateley et al. described how the rate of gas-phase deposition altered their spectra of monomeric NO due to the "flood of energy liberated by the condensing gas".[38] Again, no such difficulties were met with the experimental conditions used for the present study of allene. We suspect that the greater number of vibrational degrees of freedom for larger molecules reduces the likelihood of such problems, compared to the case of smaller molecules, by aiding in the dissipation of an energy of condensation.

4.3. Applications−Physical Properties and Reaction Chemistry. The immediate application of our work is likely to be laboratory infrared measurements on allene-containing samples, such as the determination of the column density of a neat allene ice. Perhaps more important is that with our IR band strengths it is possible for the first time to prepare *multicomponent* ices of known allene abundances because our results make possible quantitative measurements of the gas-phase deposition of allene onto a cold substrate. Just as important is the value of our near-IR results to the search for allene in Solar System ices by telescopic and spacecraft observations.

Other than the physical properties already mentioned, the vapor pressures of a wide variety of compounds have been studied for application to cometary chemistry and the sublimation of ices. Solid allene has not, to our knowledge, been examined. However, our band strengths, coupled with the method described by Khanna et al., will allow IR spectra to be used for vapor-pressure determinations and an enthalpy of sublimation.[39]

Our IR work also is capable of straightforward extension to both longer and shorter wavelengths (wavenumbers) for the far- and near-IR regions, respectively. By proper scaling and measurements, allene band strengths for both regions can be calculated. Since allene lacks a dipole moment and thus cannot be detected by radio and microwave (rotational) methods, it is likely that future spectroscopic work on this compound will involve IR measurements.

A particularly interesting application of our results concerns the reaction chemistry of Figure 8, the propyne-to-allene conversion. Propyne has been known for many years to be both an interstellar[40] and a Solar System molecule, and its formation has been investigated in both contexts. For example, the atmosphere of Saturn's largest moon, Titan, is primarily composed of N_2 and CH_4, with cosmic radiation, solar UV, and magnetospheric radiation from Saturn all initiating reactions to make a variety of hydrocarbon and nitrile products, among them propyne.[41] Low-temperature irradiation of solid CH_4, to mimic cosmic-ray bombardment, has been shown to generate propyne upon warming of the ice sample.[42]

Given that propyne is present in extraterrestrial environments, its conversion to allene is of interest, and it is a reaction that can be quantified at low temperatures with our results. Propyne-to-allene isomerization involves a 1,3-hydrogen shift, as seen in reaction 4, and has been reported in rare-gas matrices by Jacox and Milligan.[43] Our work shows that the reaction also proceeds in non-rare-gas solids.

$$H_3C{-}C{\equiv}CH \rightarrow H_2C{=}C{=}CH_2 \quad (4)$$

This reaction is analogous to the isomerizations in reactions 5 and 6, which have been investigated and documented not only in solid argon, but also in more reactive ices.[44,45]

$$H_3C{-}C{\equiv}N \rightarrow H_2C{=}C{=}NH \quad (5)$$

$$H_2N{-}C{\equiv}N \rightarrow HN{=}C{=}NH \quad (6)$$

Figure 8 gives the result of our experiment to examine the propyne-to-allene conversion, as already described. Our interpretation of the experiment is that of the propyne destroyed, about 10% went to allene formation. This value may change after additional work, but for now the importance is not so much the exact value as that for the first time a numerical value can be obtained at all. Of reactions 4−6, only for reaction 4 can a yield be directly measured in the solid state, as the product is readily available and easily handled, unlike the products in reactions 5 and 6. Going further, given the ease with which reactions 4−6 occur in laboratory ices, there is little reason to doubt that these reactions also will occur by photo- and radiation-chemical paths in interstellar and Solar System ices. The four reactants and products in reactions 5 and 6 are known to be interstellar molecules, as is propyne in reaction 4, suggesting that propyne in an extraterrestrial environment will be accompanied by allene, provided sufficient photo- or radiation-chemical initiators are present.

Turning from allene's formation to its reactions, one interesting possibility is O atom capture. Singmaster and Pimentel examined the reactions of O atoms with allene to give allene oxide, a cyclic compound,[46] which is a transformation analogous to the well-known formation of epoxides by the reaction of O atoms with alkenes. There are several

https://doi.org/10.1021/acsearthspacechem.1c00339
ACS Earth Space Chem. 2022, 6, 1163−1170

extraterrestrial O atom sources, such as CO_2, so allene oxide and its isomerization and reduction products are reasonably safe predictions. Again, our IR results can be used to determine initial abundances by IR spectroscopy and to follow the course of such allene reactions in laboratory ices.

In addition to forming allene oxide, solid allene can, of course, also revert to propyne according to

$$H_2C{=}C{=}CH_2 \rightarrow HC{\equiv}C{-}CH_3 \quad (7)$$

as shown by Jacox and Milligan.[43] Analogous reactions include reaction 8 below, again studied by Jacox and Milligan.[47]

$$HN{=}C{=}O \rightarrow N{\equiv}C{-}OH \quad (8)$$

Both the reactant and product in reaction 8 are interstellar molecules.[48,49]

5. SUMMARY AND CONCLUSIONS

In this paper we have presented IR spectra of the amorphous and crystalline forms of solid allene under vacuum at 8 and 80 K, respectively. We also have presented measurements of two forms of IR intensity, absorption coefficients (α') and band strengths (A'), along with measurements of refractive indices, densities, and optical constants. The relevance of these measurements has been described and several applications have been suggested, including future work on radiation- and photochemical changes of allene in interstellar and Solar System environnments and the search for allene in Solar System ices.

AUTHOR INFORMATION

Corresponding Author

Reggie L. Hudson − *Astrochemistry Laboratory, NASA Goddard Space Flight Center, Greenbelt, Maryland 20771, United States;* orcid.org/0000-0003-0519-9429; Email: reggie.hudson@nasa.gov

Author

Yukiko Y. Yarnall − *Astrochemistry Laboratory, NASA Goddard Space Flight Center, Greenbelt, Maryland 20771, United States; Universities Space Research Association, Greenbelt, Maryland 20771, United States*

Complete contact information is available at: https://pubs.acs.org/10.1021/acsearthspacechem.1c00339

Notes

The authors declare no competing financial interest.

ACKNOWLEDGMENTS

This project was initiated with NASA funding through the Cassini Data Analysis Program. Recent support from NASA's Planetary Science Division Internal Scientist Funding Program through the Fundamental Laboratory Research (FLaRe) work package at the NASA Goddard Space Flight Center is acknowledged. Y.Y.Y. thanks the NASA Postdoctoral Program for her fellowship. Many of the IR spectra used in this project were recorded by Ryan Coones (University of Reading, UK) and Perry Gerakines (NASA Goddard Space Flight Center). The latter is particularly thanked for assistance with software for our error analyses.

REFERENCES

(1) Gerakines, P. A.; Hudson, R. L. Infrared Spectra and Optical Constants of Elusive Amorphous Methane. *Astrophys. J.* **2015**, *805*, L20.

(2) Hudson, R. L.; Gerakines, P. A.; Moore, M. H. Infrared Spectra and Optical Constants of Astronomical Ices: II. Ethane and Ethylene. *Icarus* **2014**, *243*, 148.

(3) Hudson, R. L.; Ferrante, R. F.; Moore, M. H. Infrared Spectra and Optical Constants of Astronomical Ices: I. Amorphous and Crystalline Acetylene. *Icarus* **2014**, *228*, 276.

(4) Hudson, R. L.; Yarnall, Y. Y.; Gerakines, P. A.; Coones, R. T. Infrared Spectra and Optical Constants of Astronomical Ices: III. Propane, Propylene, and Propyne. *Icarus* **2021**, *354*, 114033.

(5) Lombardo, N. A.; Nixon, C. A.; Greathouse, T. K.; Bézard, B.; Jolly, A.; Vinatier, S.; Teanby, N. A.; Richter, M. J.; Irwin, P. J. G.; Coustenis, A.; Flasar, F. M. Detection of Propadiene on Titan. *Astrophys. J.* **2019**, *881*, L33.

(6) Linnett, J. W.; Avery, W. H. Infra-red and Raman Spectra of Polyatomic Molecules. IV. Allene. *J. Chem. Phys.* **1938**, *6*, 686.

(7) Lord, R. C.; Venkateswarlu, P. The Rotation-Vibration Spectra of Allene and Allene-d_4. *J. Chem. Phys.* **1952**, *20*, 1237.

(8) Blanc, J.; Brecher, C.; Halford, R. S. Motions of Molecules in Condensed Systems. XII. Infrared Spectrum and Structure of a Single Crystal of Allene. *J. Chem. Phys.* **1962**, *36*, 2654.

(9) Moore, M. H.; Ferrante, R. F.; Moore, W. J.; Hudson, R. L. Infrared Spectra and Optical Constants of Nitrile Ices Relevant to Titan's Atmosphere. *Astrophys. J. Supp. Ser.* **2010**, *191*, 96.

(10) Hudson, R. L.; Loeffler, M. J.; Gerakines, P. A. Infrared Spectra and Band Strengths of Amorphous and Crystalline N_2O. *J. Chem. Phys.* **2017**, *146*, No. 024304.

(11) Hollenberg, J. L.; Dows, D. A. Absolute Infrared Intensities in Crystalline Benzene. *J. Chem. Phys.* **1962**, *37*, 1300.

(12) Heavens, O. S. *Optical Properties of Thin Solid Films*, 2nd ed.; Dover, New York, 2011; p 114.

(13) Tempelmeyer, K. E.; Mills, D. W. Refractive Index of Carbon Dioxide Cryofrost. *J. Appl. Phys.* **1968**, *39*, 2968.

(14) Groner, P.; Stolkin, I.; Günthard, H. H. Measurement of Deposition Rate in Matrix Spectroscopy with a Small Laser. *J. Phys. E. - Sci. Instrum.* **1973**, *6*, 122.

(15) Wood, B. E.; Smith, A. M. *Infrared reflectance and refractive index measurements in a vacuum-rated hemiellipsoidal mirror reflectometer from 20 to 300 K*; Technical Report AEDC-TR-81-21; ARO, Inc.: Arnold Air Force Station, TN, 1981.

(16) Malherbe, F. E.; Bernstein, H. J. Infrared Spectra of Rapidly Solidified Vapors. *J. Chem. Phys.* **1951**, *19*, 1607.

(17) Hudson, R. L.; Gerakines, P. A.; Ferrante, R. F. IR Spectra and Properties of Solid Acetone, an Interstellar and Cometary Molecule. *Spectrochim. Acta* **2018**, *193*, 33.

(18) Hudson, R. L.; Yarnall, Y. Y.; Coleman, F. M. Infrared Spectra and Other Properties of Amorphous and Crystalline Dimethyl Ether. *Spectrochim. Acta* **2020**, *233*, 118217.

(19) Hollenberg, J. L.; Dows, D. A. Measurement of Absolute Infrared Absorption Intensities in Crystals. *J. Chem. Phys.* **1961**, *34*, 1061.

(20) Irvin, J. A.; Quickenden, T. I. Linear Least Squares Treatment When There are Errors in Both x and y. *J. Chem. Educ.* **1983**, *60*, 711.

(21) Press, W. H.; Teukolsky, S. A.; Vetterline, W. T.; Flannery, B. P. *Numerical Recipes in FORTRAN*, 2nd ed.; Cambridge, 1992; p 660.

(22) Hudgins, D. M.; Sandford, S. A.; Allamandola, L. J.; Tielens, A. G. G. M. Mid- and Far-Infrared Spectroscopy of Ices: Optical Constants and Integrated Absorbances. *Astrophys. J. Supp. Ser.* **1993**, *86*, 713.

(23) Luna, R.; Molpeceres, G.; Ortigoso, J.; Satorre, M. A.; Domingo, M.; Maté, B. Densities, Infrared Band Strengths, and Optical Constants of Solid Methanol. *Astron. & Astrophys.* **2018**, *617*, A116.

(24) Gerakines, P. A.; Hudson, R. L. A Modified Algorithm and Open-Source Computational Package for the Determination of

Infrared Optical Constants Relevant to Astrophysics. *Astrophys. J.* **2020**, *901*, 52.
(25) Gerakines, P. A.; Hudson, R. L. First Infrared Band Strengths for Amorphous CO_2, an Overlooked Component of Interstellar Ices. *Astrophys. J.* **2015**, *808*, L40.
(26) Hudson, R. L.; Gerakines, P. A.; Loeffler, M. Activation of Weak IR Fundamentals of Two Species of Astrochemical Interest in the T_d Point Group - The Importance of Amorphous Ices. *Phys. Chem. Chem. Phys.* **2015**, *17*, 12545.
(27) Halford, R. S.; Schaeffer, O. A. Motions in Condensed Systems II. The Infra-Red Spectra for Benzene Solid, Liquid, and Vapor in the Range from 3 to 16.7 μ. *J. Chem. Phys.* **1946**, *14*, 141.
(28) Es-sebbar, Et; Jolly, A.; Benilan, Y.; Farooq, A. Quantitative and Mid-Infrared Spectra of Allene and Propyne from Room to High Temperatures. *J. Mol. Spectrosc.* **2014**, *305*, 10.
(29) Yamada, H.; Person, W. B. Absolute Infrared Intensities of Fundamental Absorption Bands in Solid CO_2 and N_2O. *J. Chem. Phys.* **1964**, *41*, 2478.
(30) Ovchinnikov, M. A.; Wight, C. A. Inhomogeneous Broadening of Infrared and Raman Spectral Bands of Amorphous and Polycrystalline Thin Films. *J. Chem. Phys.* **1993**, *99*, 3374.
(31) Ovchinnikov, M. A.; Wight, C. A. Infrared Line Shapes of Clusters and Microcrystals: Vibrational Modes Mixed by Dipole Interactions. *J. Chem. Phys.* **1994**, *100*, 972.
(32) Taj, S.; Baird, D.; Rosu-Finsen, A.; McCoustra, M. R. S. Surface Heterogeneity and Inhomogeneous Broadening of Vibrational Line Profiles. *Phys. Chem. Chem. Phys.* **2017**, *19*, 7990.
(33) Ferrante, R. F.; Moore, M. H.; Spiliotis, M. M.; Hudson, R. L. Formation of Interstellar OCS: Radiation Chemistry and IR Spectra of Precursor Ices. *Astrophys. J.* **2008**, *684*, 1210.
(34) Ovchinnikov, M. A.; Wight, C. A. Dipole Mechanism of Line Broadening in Amorphous Solids. *J. Chem. Phys.* **1995**, *102*, 67.
(35) Mizuno, Y.; Kofu, M.; Yamamuro, O. X-Ray Diffraction Study of Simple Molecular Glasses Created by Low-Temperature Vapor Deposition. *J. Phys. Soc. Jpn.* **2016**, *85*, 124602.
(36) Takeda, K.; Oguni, M.; Suga, H. A DTA Apparatus for Vapor-Deposited Samples - Characterization of Some Vapor-Deposited Hydrocarbons. *Thermochim. Acta* **1990**, *158*, 195.
(37) Jacox, M. E. Solid-State Vibrational Spectra of Ethylene and Ethylene-d_4. *J. Chem. Phys.* **1962**, *36*, 140.
(38) Fateley, W. G.; Bent, H. A.; Crawford, B., Jr. Infrared Spectra of the Frozen Oxides of Nitrogen. *J. Chem. Phys.* **1959**, *31*, 204.
(39) Khanna, R. K.; Allen, J. E., Jr.; Masterson, C. M.; Zhao, G. Thin-Film Infrared Spectroscopic Method for Low-Temperature Vapor-Pressure Measurements. *J. Phys. Chem.* **1990**, *94*, 440.
(40) Snyder, L. E.; Buhl, D. Interstellar Methylacetylene and Isocyanic Acid. *Nature Phys. Sci.* **1973**, *243*, 45.
(41) Maguire, W. C.; Hanel, R. A.; Jennings, D. E.; Kunde, V. G.; Samuelson, R. E. C_3H_8 and C_3H_4 in Titan's Atmosphere. *Nature* **1981**, *292*, 683.
(42) Abplanalp, M. J.; Góbi, S.; Kaiser, R. I. On the Formation and the Isomer Specific Detection of Methylacetylene (CH_3CCH), Propene (CH_3CHCH_2), Cyclopropane (c-C_3H_6), Vinylacetylene (CH_2CHCCH), and 1,3-Butadiene ($CH_2CHCHCH_2$) from Interstellar Methane Ice Analogues. *Phys. Chem. Chem. Phys.* **2019**, *21*, 5378.
(43) Jacox, M. E.; Milligan, D. E. Matrix-Isolation Study of Vacuum Ultraviolet Photolysis of Allene and Methylacetylene - Vibrational and Electronic Spectra of Species C_3, C_3H, C_3H_2, and C_3H_3. *Chem. Phys.* **1974**, *4*, 45.
(44) Hudson, R. L.; Moore, M. H. Reactions of Nitriles in Ices Relevant to Titan, Comets, and the Interstellar Medium: Formation of Cyanate Ion, Ketenimines, and Isonitriles. *Icarus* **2004**, *172*, 466.
(45) Duvernay, F.; Chiavassa, T.; Borget, F.; Aycard, J.-P. Carbodiimide Production from Cyanamide by UV Irradiation and Thermal Reaction on Amorphous Water Ice. *J. Phys. Chem. A* **2005**, *109*, 603.
(46) Singmaster, K. A.; Pimentel, G. C. Photolysis of Allene Ozone Mixtures at 647 nm in Cryogenic Matrices. 1. Formation of Allene Oxide. *J. Mol. Struct.* **1989**, *194*, 215.
(47) Jacox, M. E.; Milligan, D. E. Low-Temperature Infrared Study of Intermediates in Photolysis of HNCO and DNCO. *J. Chem. Phys.* **1964**, *40*, 2457.
(48) Snyder, L. E.; Buhl, D. Interstellar Isocyanic Acid. *Astrophys. J.* **1972**, *177*, 619.
(49) Brünken, S.; Gottlieb, C. A.; McCarthy, M. C.; Thaddeus, P. Laboratory Detection of HOCN and Tentative Identification in Sgr B2. *Astrophys. J.* **2009**, *697*, 880.

https://doi.org/10.1021/acsearthspacechem.1c00339
ACS Earth Space Chem. 2022, 6, 1163−1170